2012 TO Meeting

Characterizing the Arauco Barrier Effect

Yu-nung Nina Lin[1], Anthony Sladen[1], Francisco Ortega-Culaciati[1], Mark Simons[1], Jean-Philippe Avouac[1], Eric J. Fielding[2], Benjamin A. Brooks[3], Michael Bevis[4], Jeff Genrich[1], Andreas Rietbrock[5], Christophe Vigny[6], Robert Smalley[7], and Anne Socquet[8]

1. Division of Geological and Planetary Sciences, California Institute of Technology
2. Jet Propulsion Laboratory, California Institute of Technology
3. Institute of Geophysics and Planetology, University of Hawaii
4. School of Earth Sciences, Ohio State University
5. Department of Earth and Ocean Sciences, University of Liverpool, United Kingdom
6. Département Terre Atmosphère Océan, École Normale Supérieure, Paris, France
7. University of Memphis
8. Université Joseph Fourier

ABSTRACT

Constraining the spatial heterogeneity in frictional properties on major faults and the characteristics of inferred barriers are key steps to understanding the rupture processes of large earthquakes. Observations of coseismic and postseismic deformation associated with the 2010 Mw=8.8 Maule earthquake in south-central Chile offer an opportunity to serve this goal. We find the bulk of the coseismic slip within a single elongated patch 460-km long and 100-km wide at depths between 15 and 40 km. We derive three major afterslip patches: one extends northwards along strike as well as down-dip of the major coseismic patch between 40 and 60 km depth; the other two bound the northern and southern ends of the coseismic patch. The southern patch offshore of the Arauco Peninsula is the only place showing resolvable afterslip shallower than 20-km depth. The potency released by the postseismic slip in the 1.3 years following the earthquake amounts to 20-30% of that released coseismically. Our estimates of the frictional properties show that the Arauco Peninsula area has low positive $(a-b)\sigma_n$ values, 0.01~0.22 MPa, suggesting that dynamic ruptures can propagate into the area. The uplift of the Arauco Peninsula area since 1835 cannot be fully compensated by elastic interseismic subsidence, indicating coseismic and postseismic effects may be responsible for uplift. The Arauco Peninsula area, being the termination or initiation zone of multiple ruptures, could owe its barrier effect not so much to its modest rate-strengthening effect but to the relative large spatial extent of the inferred rate-strengthening zone.

SEISMOTECTONIC & GEOLOGICAL SETTINGS

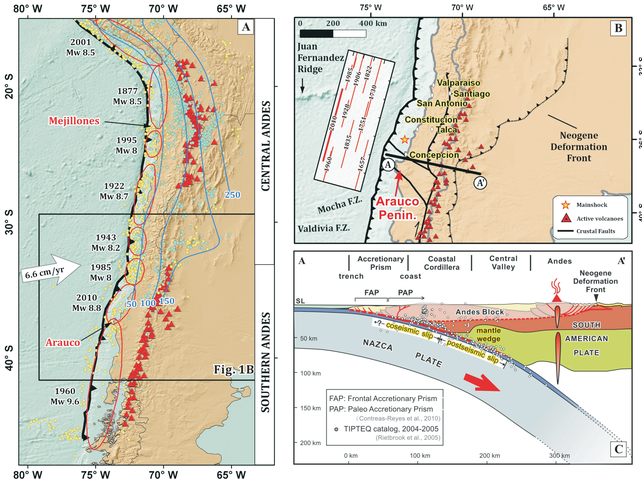

Figure 1 (A) Regional tectonic map showing slab isodepth contours (blue lines) [Cahill and Isacks, 1992], M>=4 earthquakes from NEIC catalog between 1976 and 2011 (yellow circles for depths less than 50 km, and blue circles for depths greater than 50 km), active volcanoes (red triangles), and the approximate extent of large megathrust earthquakes during the past hundred years (red ellipses) adapted from Campos et al. [2002]. The large white vector represents the direction of Nazca Plate with respect to stable South America [Kendrick et al., 2003]. (B) Simplified seismo-tectonic map of the study area. Major Quaternary faults are adapted after Melnick et al. [2009] (black lines). The Neogene Deformation Front is adapted from Folguera et al. [2004]. The west-vergent thrust fault that bounds the west of the Andes between 32° and 38°S is adapted from Melnick et al. [2009]. (C) Schematic cross-section along line A-A' (Fig. 1B), adapted from Folguera and Ramos [2009]. The upper bound of the coseismic slip coincides with the boundary between the frontal accretionary prism and the paleo-accretionary prism [Contreras-Reyes et al., 2010], whereas the contact between the coseismic and postseismic patch is from this study. The thick solid red line and dashed red line on top of the slab represent the approximate coseismic and post- plus interseismic section of the subduction interface. The thin red and grey lines are active and inactive structures in the retroarc, adapted from Folguera and Ramos [2009]. The red dashed line underneath the Andean Block represents the regional décollement.

GPS & InSAR OBSERVATIONS

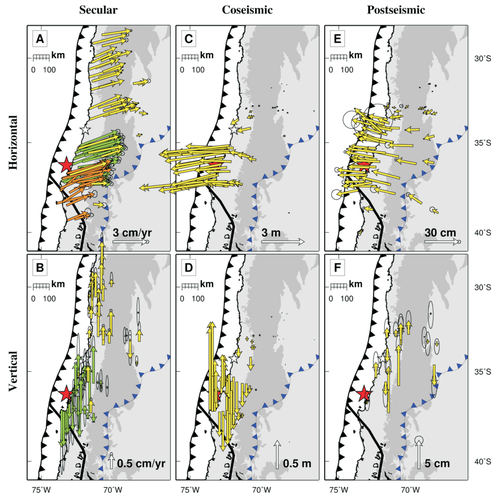

Figure 2 Horizontal and vertical secular interseismic velocities (left), coseismic displacement (middle) and postseismic displacement spanning the period between the 1st and 488th day after the mainshock (right). Note that for the postseismic displacement, when actual data time span for a given record does not cover this whole period, we have extrapolated it to represent the deformation between the 1st and 488th day using PCAIM,. Yellow vectors are derived from this study; green vectors and orange vectors in (A) and (B) are from are from Ruegg et al. [2009] and Moreno et al. [2008], respectively. The blue barbed line corresponds to the Neogene Deformation Front. The red and white stars represent the epicenter of the mainshock and the Pichilemu earthquake, respectively. The dark grey region is bounded by the 1000-m contour line, approximately the boundary of the Andes.

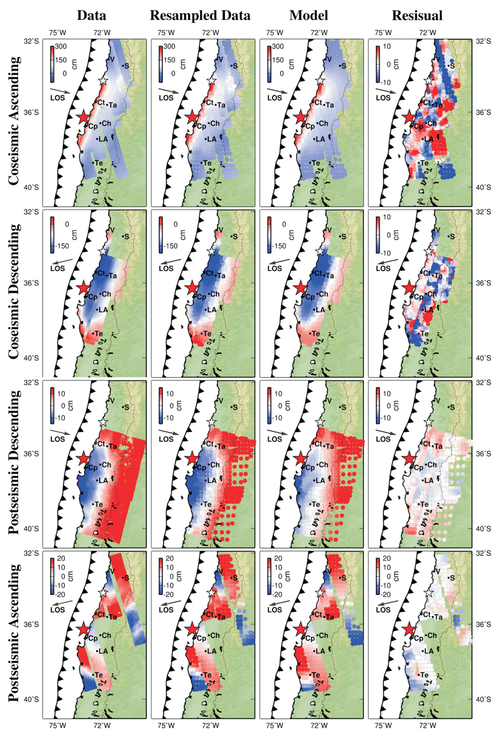

Figure 3 The original, resampled, modeled InSAR data, and the model residuals for both the coseismic and postseismic tracks. Red and white stars are for the Maule and Pichilemu earthquakes, respectively.

AFTERSLIP OF THE 2010 Mw=8.8 MAULE EARTHQAUKE

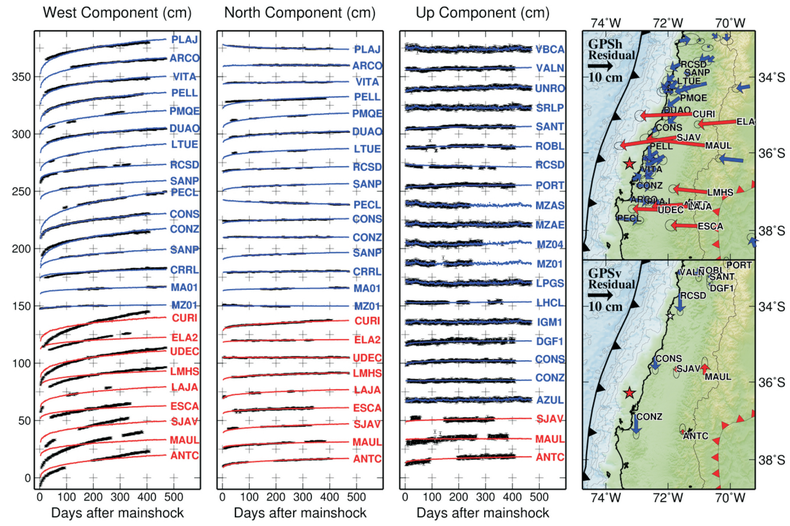

Figure 4 Time series of selected GPS stations. Blue lines and stations represent predicted time series that agree well with the data (black dots), whereas red lines and stations represent model prediction displaying large discrepancies with the data. The map views at the right panel show the residual vectors between the observed and modeled GPS components. The red stations are distributed along the Andes, indicating that the large systematic residuals are likely due to a common source.

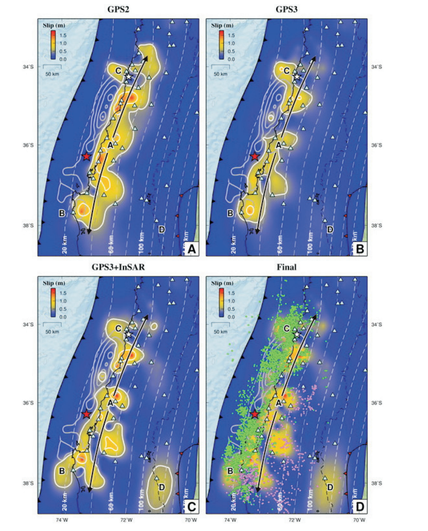

Figure 5 Comparison of the postseismic slip model between the 1st and 488th day constrained by (A) horizontal GPS observations only, (B) all three components of GPS observations, and (C) three component GPS observations plus InSAR data. Thick white contours for the afterslip are of 0.5-m intervals, and the coseismic slip model is of 2.5-m contour intervals (gray lines). The final model in (D) is the same as (C) without the afterslip contours. Green circles are aftershocks [Rietbrock et al., 2012] and pink circles are background seismicity on the megathrust (from March to June in 1996 [Campos et al., 2002] and November 2004 to October 2005 [Rietbrock et al., 2005]). Light blue triangles represent the location of GPS stations. A, B, and C correspond to regions with the most significant afterslip; black arrows indicate the elongated region of patch A.

THE ARAUCO BARRIER EFFECT

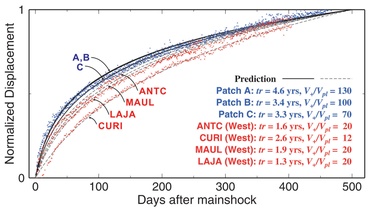

◀ **Figure 6** Normalized time-dependent displacement over different postseismic slip patches from our model result (blue dots; see Fig. 12D for locations). The normalized westward displacements over selected GPS stations are also shown for comparison (red dots; see Fig. 11 for locations). Solid and dashed black lines are the model prediction [Perfettini et al., 2010] for the former and later time series, respectively.

	A (down-dip)	B (Arauco)	C (San Antonio)
$(a-b)\sigma_n$	0.08-0.62	0.01-0.22	0.04-0.65

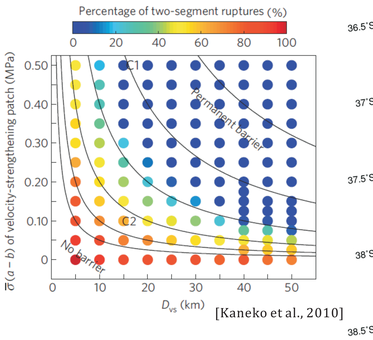

▶ **Figure 7** The barrier effect of a rate-strengthening patch scales with the product of $(a-b)\sigma_n$ and the size of the patch, based on the dynamic modeling of slip on a fault with heterogeneous rate-and-state friction patches [Kaneko et al. 2010]. It might be argued that because of a relatively small value of $(a-b)\sigma_n$ in the Arauco Peninsula area, dynamic ruptures can propagate into the area but do not rupture through it because of its relatively large size. This effect might explain why we observed both some co-seismic slip and aseismic afterslip beneath the Arauco Peninsula area.

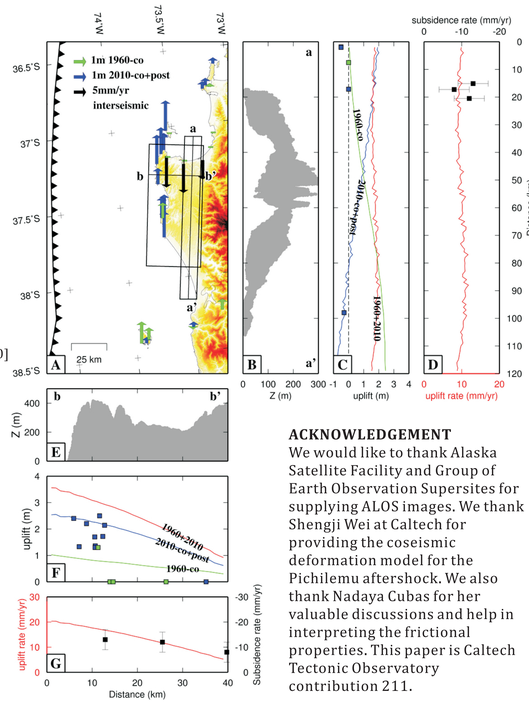

▶ **Figure 8** Topography, deformation and uplift/subsidence rate of the Arauco Peninsula along E-W and N-S directions. (A) Map of the Arauco Peninsula. a-a' and b-b' indicate locations of the profiles, with the bounding boxes showing the area of topography being projected onto the profiles. Green vectors and blue vectors are the in-situ measurements of coseismic and early postseismic vertical displacement from the 1960 Valdivia earthquake [Plafker and Savage,1970] and the 2010 Maule earthquake [Vargas et al., 2011]. Black vectors are the vertical velocities from campaign-mode GPS between 1996 and 2002 [Ruegg et al., 2009]. (B) Topography along profile a-a'. The anticlinal deformation with a WNW-SES trending axis is discussed by Melnick et al. [2009]. (C) Coseismic uplift due to the 1960 Valdivia earthquake (green line, Moreno et al. [2009]), and the coseismic plus postseismic uplift of the 2010 Maule earthquake (blue line, this study) projected along profile a-a', and the total uplift (red line). Squares are the projected in-situ measurements with the same color codes as (A). Dashed black line indicates the location of the neutral line. (D) The equivalent uplift rate (red line), derived by dividing the total uplift in (C) by the period between 2010 and 1835, assuming the year of 1835 is the onset of another seismic cycle. Black squares are the projected GPS vertical velocities. (E) Topography along the b-b' profile, showing clear back-tilting of the peninsula. (F) Uplift curves along the b-b' profile, with the same color codes as (C). (G) The equivalent uplift rate and GPS vertical velocities projected along profile b-b'.

ACKNOWLEDGEMENT

We would like to thank Alaska Satellite Facility and Group of Earth Observation Supersites for supplying ALOS images. We thank Shengji Wei at Caltech for providing the coseismic deformation model for the Pichilemu aftershock. We also thank Nadaya Cubas for her valuable discussions and help in interpreting the frictional properties. This paper is Caltech Tectonic Observatory contribution 211.